

**SCREENING OF ANTIPARASITIC COMPOUNDS FOR THYMIDYLATE SYNTHASE  
FROM *TRICHINELLA SPIRALIS*: EXTENSIVE VIRTUAL SCREENING AND  
MOLECULAR MODELING STUDIES**Lakshminarayanan Karthik\*<sup>1</sup> and Ummu Kulsu T. S.<sup>1</sup><sup>1</sup>Precision Therapeutics Laboratory, Quick IsCool, Aitele Research LLP, Bihar, India.

\*Corresponding Author: Lakshminarayanan Karthik

Precision Therapeutics Laboratory, Quick IsCool, Aitele Research LLP, Bihar, India.

Article Received on 15/06/2024

Article Revised on 05/07/2024

Article Accepted on 26/07/2024

**ABSTRACT**

*Trichinella spiralis* (*T. spiralis*), a parasitic nematode responsible for human trichinellosis, poses a significant threat to global health. Thymidylate synthase (TS) plays a crucial role in DNA synthesis and repair, making it an attractive target for drug development against this parasite. In this context, the present study aimed to identify potential small-molecule TS inhibitors in *T. spiralis* and evaluate their binding affinity through docking studies. To achieve this goal, we first conducted a comprehensive screening of chemical libraries to identify potential TS inhibitors using several small-molecule databases. Subsequently, we performed extensive docking studies to investigate the binding interactions between these compounds and the active site of TS, providing insights into their potential mechanisms of action. Our findings highlight several promising small molecules that exhibit high binding energy and strong binding affinities toward *T. spiralis* TS, suggesting their potential as novel therapeutic agents against trichinellosis. Furthermore, a comprehensive analysis of physicochemical and pharmacokinetic properties was also performed for the identified hits from each library. Ultimately, this study contributes to ongoing efforts to combat *T. spiralis* infections and underscores the importance of targeting essential enzymes such as TS as a strategy for parasite control.

**KEYWORDS:** Virtual screening docking; ADMET analysis; *Trichinella spiralis*; Thymidylate synthase; Rheedioxanthone B; PyRx docking.

**INTRODUCTION**

Nematodes encompass types of species called "parasites", which are common infectious agents and are found predominantly in developing countries.<sup>[1]</sup> These parasitic worms, such as roundworms, hookworms, and whipworms, tend to thrive in areas with insufficient hygiene and limited access to water.<sup>[2]</sup> Infections can result in a range of health issues, from discomfort to severe malnutrition and developmental challenges for individuals. Generally, infection is described as the infiltration and growth of microorganisms in tissues that can go unnoticed or cause localized cell damage due to the metabolic activity of toxins, intracellular replication, or an immune response involving antigens and antibodies. The process of infection appears to involve a series of events that ultimately lead to tissue damage in the host and, potentially, host destruction if left unnoticed.<sup>[3]</sup> It has been well established that infections can occur through several factors, such as surrounding air (airborne transmission), a living organism acting as a vector (vector-borne transmission), or even an inanimate object (vehicle-borne transmission). Incidentally, many health and governmental organizations tend to categorize these infectious diseases as either "directly" transmitted

(e.g., through sexual contact, vertical transmission, or skin-to-skin contact) or "indirectly" transmitted (e.g., through airborne, vector-borne, vehicle-borne, waterborne, or foodborne routes).<sup>[4]</sup>

The terms trichinellosis, trichinosis, and trichiniasis all allude to diseases associated with the larval and adult phases of a parasitic nematode that represents the genus *Trichinella*. The significant highlights of this disease are that it is zoonotic and that the infective hatchlings are meat borne (ordinarily pork but progressively other creature meats). Interestingly, in rare cases, the vertebrate host can also act as both an intermediate and definitive host for the parasite.<sup>[5]</sup> As a result, reproduction may occur when both the reproducing adult worms and the infective larvae develop within the same host. At present, eight species of *Trichinella* have been identified, and in addition to infected pork meat, other affected herbivores, such as sheep, goats, and cattle, have also become sources of outbreaks of trichinellosis.<sup>[6]</sup>

A comprehensive understanding of *T. spiralis* and its life cycle is vital for the development of effective preventive measures and treatments. The onset of infection

predominantly results from consuming *T. spiralis*-infected pork meat.<sup>[6]</sup> Upon infecting the host and following mating in the host's small intestine, the muscle hatchlings that develop from the newborn larvae are subsequently released by female parasites.<sup>[7]</sup> This process involving larval development within the muscles is typically completed approximately 20 days after the disease has started. Following this, the newborn larvae quickly leave the lumen and travel through the circulatory system until they reach a skeletal muscle fiber. Once inside the cytoplasm of the myofiber, the newborn larvae initiate a remodeling process. Over the next few weeks, this process transforms the myofiber into a new structure known as the 'nurse cell'.<sup>[7]</sup> During this transformation, myofibers undergo significant changes, drastically altering their transcriptome, proteome, and cellular architecture. Parasitized fibers produce angiogenic factors such as vascular endothelial growth factor, leading to the formation of new blood vessels that create a network around the fiber. In the final stages, collagens (types IV and VI) and other extracellular matrix proteins are synthesized, forming a capsule around the nurse cell. The resulting complex of nurse cells and resident nematodes becomes stable and can survive for extended periods in hosts with functioning immune systems.<sup>[7]</sup>

### Thymidylate Synthase as a Drug Target

Thymidylate synthase (TS; EC 2.1.1.45) catalyzes the reductive methylation of deoxyuridine monophosphate (dUMP) by N5,10-methylenetetrahydrofolate (meTHF) to produce thymidine monophosphate (dTMP) and dihydrofolate.<sup>[8]</sup> Understanding the functional nature of the nematode TS can be exceptionally valuable for developing novel medications for pathogenic species. As the response is the last step of the sole dTMP, which is fundamental for DNA combination, and furthermore, for cell division and endurance, the TS is a significant chemical objective in chemotherapy. Moreover, dTMP also functions as a precursor for the production of deoxythymidine triphosphate (dTTP), which in turn is further incorporated into DNA.<sup>[9]</sup> As TSs are the sole source of dTMP for *de novo* synthesis and are considered essential enzymes in DNA synthesis, they have been extensively studied for the design of anticancer compounds.<sup>[10]</sup> However, following several reports confirming the presence of TS in nematodes, such as *Angiostrongylus cantonensis*, *T. pseudospiralis*, and *T. spiralis*, TSs have also been considered potent drug targets for identifying and developing novel antimalarial and antiparasitic drugs.<sup>[11]</sup> In addition, the following protozoan species, viz., *Crithidia fasciculata* and *C. oncopelti*, along with *Trypanosoma brucei*, *T. congolense*, *T. lewisi* (blood forms), and *T. cruzi* (intracellular and culture forms), were reported to possess TS activity. When the enzymatic activity of these parasites was compared with that of their mammalian counterparts, TSs from the parasitic species exhibited relatively greater molecular weights (175 kDa–200 kDa),

which were nearly threefold greater than those of mammalian TSs.<sup>[10]</sup>

It is widely reported that TS can function both as an enzyme and a regulator, making it a dual-function protein. Since it has been known to catalyze the reductive methylation of dUMP to dTMP, TS is considered a catalytic protein. Moreover, as TS is involved in the synthesis of proteins that help regulate the apoptotic process, it is further referred to as a regulatory protein.<sup>[12]</sup> A new related finding of potential importance is that TSs seem to have an onco-gene-like function.<sup>[13]</sup> Taken together with its critical role in nucleotide biosynthesis and other associated roles, TS has emerged as a promising drug target for various infectious diseases, including those caused by parasites such as *T. spiralis*. Based on these findings, the present study explored the importance of TS as a drug target and its potential for identifying potent antiparasitic compounds.

## MATERIALS AND METHODS

### Protein Preparation

The crystal structure of the drug target (PDB ID: 5M4Z) was retrieved from the Protein Data Bank. The ligand in the protein structure was permanently removed prior to starting the virtual screening docking. In addition, polar hydrogens were incorporated into the protein structure, and the atoms that make up the protein were assigned Kohlman charges. This phase is crucial throughout the docking process because it ensures the accurate representation of electrostatic interactions. Furthermore, prior to the docking process, all water molecules, other co-crystallized ligands and typical protein structure artifacts were also removed. Commonly, this method is used to speed up the docking process and simplify computations.

### Selection of Lead Compounds and Construction of Small Molecule Libraries

Parasitic infections have long posed a significant threat to public health, but there are few effective treatments available for parasitic infections. It has long been recognized that the enzyme TS, which is involved in nucleotide biosynthesis, could be a target for stopping parasitic growth. As a potential source of new antiparasitic targets, this enzyme, which involves intricate interactions, has been the subject of extensive research.<sup>[14–16]</sup> From an extensive literature review, the following three compounds: “1-(2-methylpropyl)-4-(5-thiophen-2-yl-1H-imidazol-2-yl), pyrrolidin-2-one” 9 (CID-45242586), “1-(2-deoxy-5-O-phosphonopentofuranosyl)-5-fluoro-4-(hydroxyamino)pyrimidin-2(1H)-one (N(4)-OH-5-Fdcmp)”, and “Rheediaxanthone B” were identified as the lead compounds for subsequent molecular docking studies (Figure 1).<sup>[17–18]</sup> Furthermore, compounds structurally similar to these three compounds were identified via searches of the PubChem and Binding databases. Among these repositories, a significant

number of hits—i.e., compounds conforming to Lipinski's rule of five and structurally similar to three

lead compounds—were retrieved in 3-D format from the PubChem database.

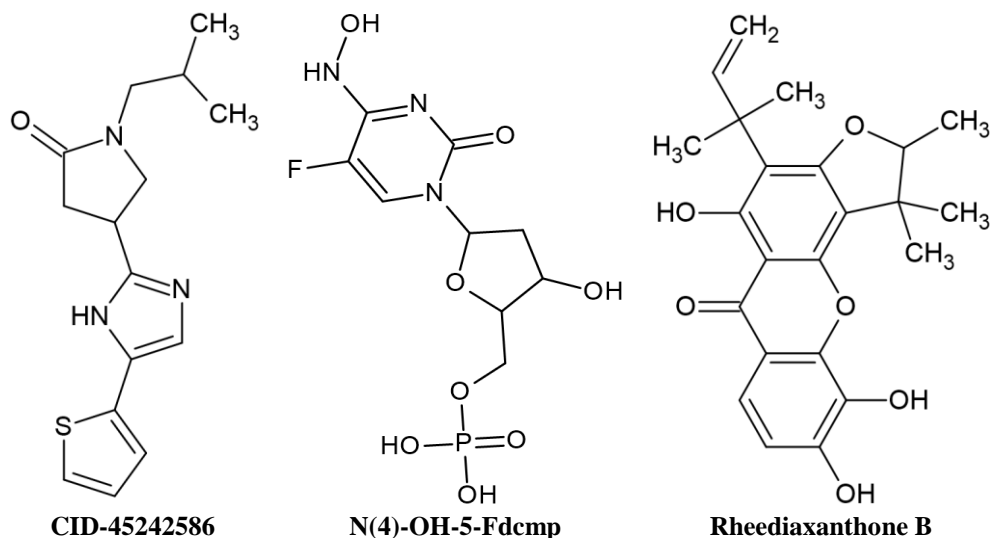


**Figure 1: 2D Chemical Diagrams of the Selected Lead Compounds.**

### Molecular Docking using PyRx

The virtual screening docking process was executed using AutoDock Vina integrated into PyRx.<sup>[19]</sup> AutoDock Vina is widely considered to be one of the most rapid and extensively employed open-source applications for molecular docking within the academic community. AutoDock Vina is a commonly used subatomic docking program utilized to predict how ligands bind to receptors or proteins. The 3D compounds of the selected libraries were acquired from PubChem in an ".sdf" file and subsequently converted to the ".pdbqt" format using Open Babel, a coordinated part of PyRx software. To perform molecular docking, a three-dimensional grid box was established with an exhaustiveness setting of eight. This approach facilitated a thorough search through numerous possible ligand conformations, resulting in accurate identification of the optimal docking position. The dimensions of the box for the target protein (PDB: 5M4Z) were meticulously set to size\_x = 55.444 Å, size\_y = 50.4955 Å, and size\_z = 9.1779 Å, creating an XYZ dimension of 54 × 57 × 55 Å. Throughout the docking process, ligands were able to adjust their conformations for optimal binding, while the target protein was treated as a rigid structure with a fixed conformation. The Discovery Studio program and ChimeraX software were used to analyze and visualize the interactions between the target protein and ligands after completion of the docking process.<sup>[20-21]</sup>

### Physicochemical and ADMET Analysis

The evaluation of physicochemical and absorption, distribution, metabolism, excretion, and toxicity (ADMET) parameters plays a crucial role in assessing the pharmacokinetic and safety profiles of compounds, especially in the context of molecular docking studies. These parameters help in understanding how well a potential drug candidate is absorbed, distributed, metabolized, and eliminated within the body, as well as

its potential toxicity. Incorporating physicochemical and ADMET analyses in combination with molecular docking studies provides a comprehensive view of a compound's suitability for further development. In the present study, we conducted a thorough evaluation of the physicochemical and ADMET properties of the higher-ranked compounds using two widely used online tools, SwissADME and pkCSM. By combining the insights gained from these platforms, a more comprehensive analysis of the compounds can be achieved. The SwissADME Web tool facilitates the calculation of essential physicochemical, pharmacokinetic, drug-like, and associated parameters for individual or multiple molecules.<sup>[22]</sup> Various key parameters, such as molecular weight, lipophilicity (logP), and water solubility, among others, were analyzed to gain valuable insights into the chemical composition of the compounds. The pkCSM approach provides a platform for the assessment and enhancement of pharmacokinetic and toxicity properties.<sup>[23]</sup> It is accessible through a user-friendly web interface (<http://structure.bioc.cam.ac.uk/pkcsml>) and serves as a valuable resource for medicinal chemists to optimize the equilibrium between potency, safety, and pharmacokinetic characteristics.

### RESULTS AND DISCUSSION

Docking scores are numerical values obtained from computational docking studies that predict how well a ligand (molecule) binds to its target protein. The larger the negative value is, i.e., the higher the binding energy is, the stronger the predicted binding affinity between the ligand and the protein. In this context, the binding energies of the top ten lead compounds obtained from each library against *T. spiralis* TS are provided in Table 1. Briefly, in the CID45242586 library, the top-ranked compounds exhibited binding energies ranging from "-8.2 to -7.1 kcal/mol". Similarly, the top-ranked compounds identified in the other libraries, "N(4)-OH-5-



Fdcmp" and "Rheediaxanthone B", demonstrated binding energies within the ranges of "-9.4 to -8.1 kcal/mol" and "-10.2 to -8.9 kcal/mol", respectively (Table 1). In addition, *T. spiralis* TS was also tested against a few

known antifungal drugs, such as "Mebendazole" and "Albenza". The results clearly showed that the binding energy of these existing drugs was relatively lower than that of the lead compounds presented in Table 1.

**Table 1: Virtual Screening Docking of Various Libraries of Compounds toward *Trichinella spiralis* Thymidylate Synthase (PDB: 5M4Z).**

Sl. No	CID45242586 Library	Binding Energy (kcal/mol)	N(4)-OH-5-Fdcmp lead compounds Library	Binding Energy (kcal/mol)	Rheedia xanthone B Library	Binding Energy (kcal/mol)	Control Drugs	Binding Energy (kcal/mol)
1	28230373	-8.2	7058166	-9.4	73205	-10.2	Mebendazole	-8.1
2	71797212	-8.0	20056867	-9.2	10342859	-10.0	Albenza	-6.3
3	97104814	-7.9	46936402	-9.1	52951054	-9.9		
4	28360425	-7.8	46937009	-8.9	195652	-9.8		
5	31054613	-7.6	25244665	-8.8	11725803	-9.7		
6	76533214	-7.5	447090	-8.7	102060338	-9.5		
7	129067958	-7.4	7058165	-8.6	10862711	-9.3		
8	45179028	-7.3	12358859	-8.5	637252	-9.2		
9	45185893	-7.2	53840688	-8.4	10342859	-9.0		
10	156276243	-7.1	25202302	-8.1	15307925	-8.9		

Furthermore, all the top-ranked compounds from the chosen libraries exhibited favorable hydrogen bonding and nonbonding interactions. While the lead compounds were found to interact with key active site residues, viz., Cys 189, Gln 208, Arg 209, and Asp 212, through hydrogen bonding interactions, they were also involved in forming nonbonded interactions with adjacent or surrounding key residues, such as Phe 74, Glu 81, Ile

102, Trp 103, Leu 186, His 190, Ser 210, Ala 211, Leu 215, Gly 216, Phe 219, and Asn 220 (Figure 2). Collectively, these virtual screening docking results suggested that the top-ranked compounds from the three libraries have promising binding affinities, indicating their potential as lead candidates for further optimization and development.

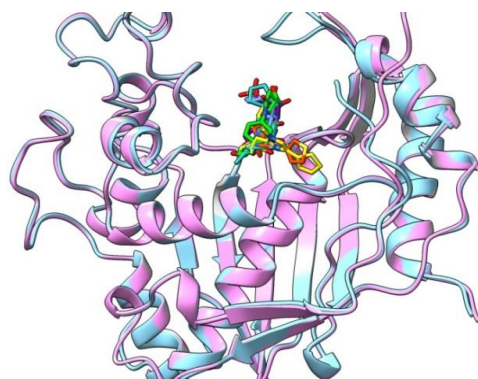


**Figure 2a**

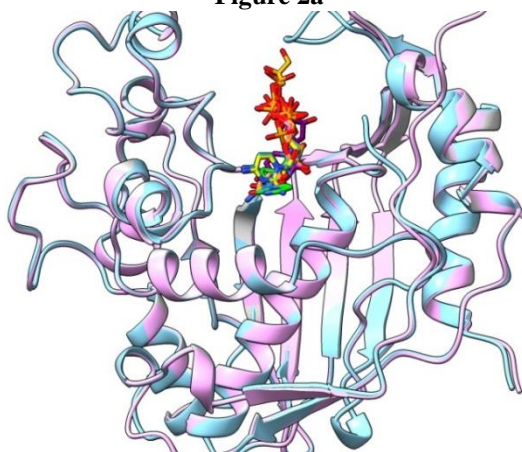


**Figure 2c**

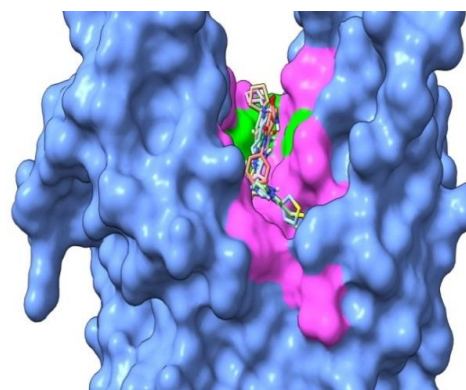


**Figure 2b**

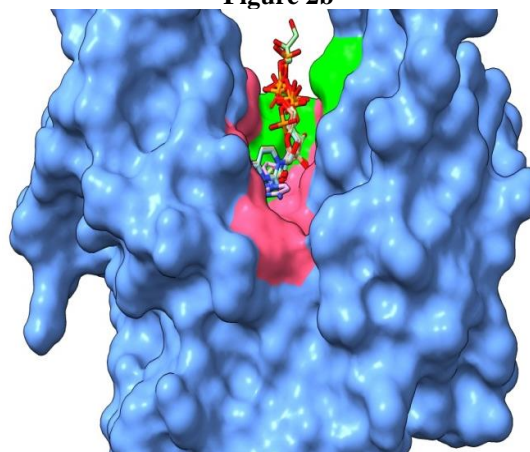


**Figure 2d**

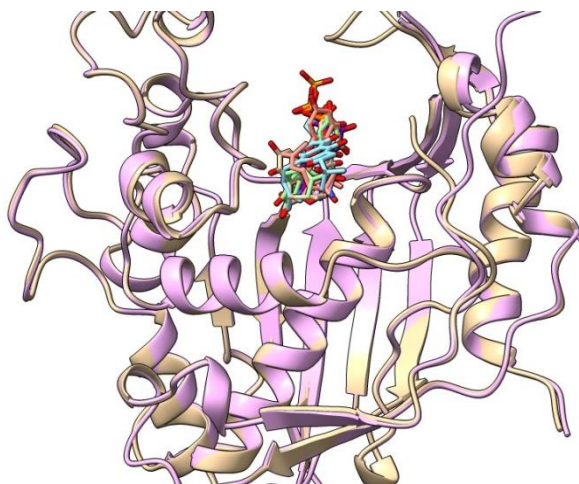


Figure 2e

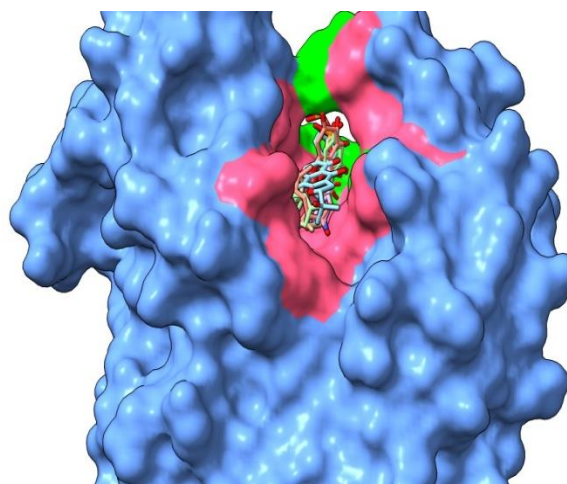


Figure 2f

Figure 2a, c, and e: Superimposed image displaying the binding of the lead compounds from CID45242586, N(4)-OH-5-Fdcmp, and Rheediaxanthone B Libraries, respectively, within the active site pocket of *T. spiralis* TS. The respective lead compounds are rendered in stick representation, whereas the target enzyme TS is rendered in ribbon representation. Figure 2b, d, and f: Surface representation of *T. spiralis* TS (as depicted in 2a, c, and e) displaying the hydrogen bond and nonbonded interactions of the lead compounds identified from the three libraries. For clarity, the interactions are not shown here. Instead, the regions exhibiting hydrogen bonding interactions are colored green, whereas the nonbonded interactions comprising van der Waals, pi-alkyl, pi-sulfur, etc., are colored pink.

#### Properties of Physicochemical and Drug Likeness

Physicochemical properties are the physical and chemical characteristics of a drug. These characteristics include the molecular weight, solubility, ionization state, and hydrogen bonding capacity of the drug. Understanding these properties is important for drug development and determining a drug's effectiveness. According to Lipinski's Rule of Five, a compound must meet certain criteria to be considered a likely drug candidate. These criteria include a molecular weight (MW) less than or equal to 500 g/mol, a hydrogen bond donor (HBD) limited to 5, a hydrogen bond acceptor (HBA) limited to 10, and a topographical polar surface area (TPSA) of no more than 140 Å<sup>2</sup>. The log Po/w (consensus) is the average of all five lipophilic predictions (iLOGP, XLOGP3, WLOGP, MLOGP, and SILICOS-IT). For a drug to be effective when taken orally, it should have a LogP value of less than 5, ideally between 1.35 and 1.8. This ensures good absorption in the intestines. To predict the aqueous solubility of a compound directly from its structure, we used log S (ESOL). The most acceptable Log S (ESOL) value is between -4 and 6. Bioavailability refers to the percentage

of a xenobiotic dose that enters the systemic circulation. The ideal bioavailability score is less than or equal to 0.55.

Veber's rule sets a high standard for bioavailability, requiring no less than 10 rotatable bonds and no more than 140 Å<sup>2</sup> of TPSA. The Ghose filter aims to improve prediction by stating that the absorption peak has the following values: MW of 160 to 480 Da, molar refractivity (A) of 40 to 130, LogP of -0.4 to 5.6, and total atomic number between 20 and 70. The Egan rule considers compounds with a TPSA ≥ 0 to ≤ 132 Å<sup>2</sup> and a LogP ≥ -1 to ≤ 6 to have good bioavailability. Muegge's rule has modified the property ranges and included the following additional parameters: MW (200–600), LogP (-2–5), PSA ≤ 150, number of rings ≤ 7, number of carbons > 4, number of heteroatoms > 1, number of rotatable bonds ≤ 15, HBD ≤ 5, and HBA ≤ 10 to differentiate between drug-like and nondrug-like compounds. In our study, the physicochemical properties of the lead compounds from various libraries were evaluated using Swiss ADME analysis.

Table 2a: Physicochemical Properties of Lead Compounds from the CID45242586 Library.

Sl.No	Compound ID	Mol.wt g/mol	HBA	HBD	TPSA (Å <sup>2</sup> )	Log Po/w (Consensus)	Log S (ESOL)	Drug likeness: Y(Yes)/N(No) (Lipinski Rules)	Bioavailability
1	28230373	303.42	2	1	77.23	2.97	-3.34	Y, 0 Violation	0.55
2	71797212	337.44	2	1	77.23	3.19	-3.77	Y, 0 Violation	0.55
3	97104814	366.48	3	1	90.12	3.13	-3.77	Y, 0 Violation	0.55
4	28360425	376.47	4	2	115.56	2.41	-3.45	Y, 0 Violation	0.55
5	31054613	394.49	3	1	95.47	2.41	-3.34	Y, 0 Violation	0.55
6	76533214	398.45	4	2	106.33	2.72	-3.46	Y, 0 Violation	0.55

7	129067958	372.53	3	2	89.26	3.09	-3.86	Y, 0 Violation	0.55
8	45179028	303.42	2	1	77.23	2.97	-3.34	Y, 0 Violation	0.55
9	45185893	327.38	3	1	77.23	3.11	-3.67	Y, 0 Violation	0.55
10	156276243	331.48	2	1	77.23	3.46	-4.06	Y, 0 Violation	0.55

Veber	Ghose	Egan	Muegge
Yes	Yes	Yes	Yes
Yes	Yes	Yes	Yes
Yes	Yes	Yes	Yes
Yes	Yes	Yes	Yes
Yes	Yes	Yes	Yes
Yes	Yes	Yes	Yes
Yes	Yes	Yes	Yes
Yes	Yes	Yes	Yes
Yes	Yes	Yes	Yes
Yes	Yes	Yes	Yes
Yes	Yes	Yes	Yes

As shown in Table 2a, compounds from the CID45242586 library satisfied all the Lipinski rule parameters with zero violations. These compounds have smaller molecular weights, moderate HBA and HBD numbers, and acceptable log Po/w values ranging from 2.41 to 3.46. In particular, as they are below the threshold of 5, the Log Po/w values of all compounds can be considered to be moderately lipophilic, which enables them to potentially cross cell membranes and the intestinal lining to enter the bloodstream. All the lead compounds exhibited acceptable Log S values (between -4 and 6) as well, indicating favorable water solubility. The use of Weber, Ghose, Egan, and Muegge filters further confirmed the drug likeness of all the lead compounds.

**Table 2b: Physicochemical Properties of Lead Compounds from the N(4)-OH-5-Fdcmp Library.**

Sl. No	Compound ID	Mol.wt g/mol	HBA	HBD	TPSA (Å <sup>2</sup> )	Log Po/w (Consensus)	Log S (ESOL)	Drug likeness: Y(Yes)/N(No) (Lipinski Rules)	Bioavailability
1	7058166	479.12	15	3	311.17	-3.72	1.10	Y,1 violation	0.11
2	20056867	400.15	12	3	252	-3.11	0.75	Y,1 violation	0.11
3	46936402	477.25	14	7	272.97	-3.56	1.04	N,2 violations	0.11
4	46937009	403.18	12	6	243.51	-3.22	0.73	N,2 violations	0.11
5	25244665	463.13	14	2	290.94	-3.07	1.19	Y,1 violation	0.11
6	447090	516.40	12	5	246.31	-2.60	0.07	N,1 violation	0.11
7	7058165	321.18	9	3	192.83	-2.48	0.38	Y,1 violation	0.11
8	12358859	483.16	15	7	299.85	-3.95	1.07	Y,1 violation	0.11
9	53840688	516.40	12	5	246.31	-2.50	0.07	N,1 violation	0.11
10	25202302	481.12	15	2	290.94	-2.79	0.44	Y,1 violation	0.11

Veber	Ghose	Egan	Muegge
No	No	No	No
No	No	No	No
No	No	No	No
No	No	No	No
Yes	No	No	No
No	No	No	No
Yes	No	No	No
No	No	No	No
No	No	No	No
No	No	No	No
Yes	No	No	No

The physicochemical properties of the lead compounds in the N(4)-OH-5-Fdcmp library are displayed in Table 2b. Except for compounds 6 and 9, the MWs of the other compounds were found to be < 500 Da. Incidentally, the numbers of HBA and HBD were found to be relatively higher than the allowed range. However, all the lead compounds possessed favorable gastrointestinal absorption and aqueous solubility, as evidenced by their Log Po/w and Log S scores. For oral bioavailability, the obtained score of 0.11 suggested that all the compounds

may lack optimal systemic circulation. Overall, while most of the compounds in this library have shown promising results for drug development, they also seem to violate Lipinski's rule in terms of HBA and HBD; hence, further studies are needed for clinical success.



**Table 2c: Physicochemical Properties of Lead Compounds from the Rheediaxanthone B Library.**

Sl. No	Compound ID	Mol.wt g/mol	HBA	HBD	TPSA (Å <sup>2</sup> )	Log Po/w (Consensus)	Log S (ESOL)	Drug likeness: Y(Yes)/N(No) (Lipinski Rules)	Bioavailability
1	73205	356.37	6	4	107.22	2.90	-4.68	Y,0 violation	0.55
2	10342859	434.44	7	3	109.36	3.69	-5.46	Y,0 violation	0.55
3	52951054	468.50	8	4	129.59	3.81	-5.72	Y,0 violation	0.55
4	195652	422.47	6	3	100.13	4.08	-5.70	Y,0 violation	0.55
5	11725803	356.37	6	4	107.22	2.90	-4.68	Y,0 violation	0.55
6	102060338	392.40	6	2	89.13	3.85	-5.56	Y,0 violation	0.55
7	10862711	420.45	6	2	89.13	3.90	-5.41	Y,0 violation	0.55
8	637252	442.50	7	5	127.45	3.61	-5.23	Y,0 violation	0.55
9	10342859	434.44	7	3	109.36	3.69	-5.46	Y,0 violation	0.55
10	15307925	392.40	6	2	89.13	3.86	-5.56	Y,0 violation	0.55

Veber	Ghose	Egan	Muegge
Yes	Yes	Yes	Yes
Yes	Yes	Yes	Yes
Yes	Yes	Yes	Yes
Yes	Yes	Yes	Yes
Yes	Yes	Yes	Yes
Yes	Yes	Yes	Yes
Yes	Yes	Yes	Yes
Yes	Yes	Yes	Yes
Yes	Yes	Yes	Yes
Yes	Yes	Yes	Yes

The results for the Rheediaxanthone B library are displayed in Table 2c. The lead compounds in this library possess promising physicochemical properties. This finding shows the potential of these compounds for use in drug development against the target enzyme TS. The compounds were tested according to Lipinski's Rule of Five, and no violations were detected, which is a good indicator of oral bioavailability. The molecular weights of the compounds ranged from 356.37 g/mol to 468.5 g/mol, which is effective for drug delivery and interaction with biological targets. The HBA and HBD numbers are within acceptable ranges, indicating that the optimum capacity for hydrogen bonding interactions is needed for binding to target proteins or receptors. The Log Po/w values of the compounds ranged from 2.9 to 4.08, indicating acceptable lipophilicity. The Log S (ESOL) values are within acceptable ranges, indicating satisfactory aqueous solubility, which is important for effective drug formulation and delivery. The application of filters such as Veber, Ghose, Egan, and Muegge further confirmed the drug likeness of these compounds, confirming their potential for development as effective drug candidates.

#### Evaluation of ADMET Properties

In nature, an ideal drug candidate should exhibit the right ADMET characteristics at a therapeutic dose in addition to adequate efficacy against the therapeutic target.<sup>[24]</sup> Hence, the following guidelines should be followed for drug candidates: a Caco2 level higher than 0.90 cm/s indicates that the drug is absorbed in the human gut. Greater than 30% intestinal absorption is regarded as a

favorable substance. Skin penetration is considered to be possible when the skin permeability "logKp" is greater than -2.5. A logBB greater than 0.3 for a particular substance is thought to penetrate the blood-brain barrier (BBB) more easily, whereas molecules with a logBB less than -1 are thought to be poorly distributed to the brain. Drugs with a CNS permeability (logPS) greater than -2 can enter the central nervous system, whereas drugs with a permeability less than -3 cannot. Cytochrome P450, the body's primary detoxifier, is concentrated in the liver. In nature, P450s consist of many isoforms, such as CYP1A2 and CYP2C9, and compounds that can bind to these enzymes may lead to drug-drug interactions or altered metabolism. Organic cation transporter 2 (OCT2) is a transporter protein that is primarily found in the kidneys and plays a crucial role in the renal clearance of drugs and endogenous compounds. Assessing a compound's potential to act as a substrate for renal OCT2 is critical because, if it is considered a substrate, the transporter can actively pump the drug into the urine, leading to increased renal clearance of the drug (lowering its therapeutic efficacy).

Toxicological studies have examined the safety of a potential compound. A positive AMES test indicates that the substance is carcinogenic due to its metabolic properties. A major safety concern in drug development is hepatotoxicity, which refers to the presence or absence of drug-induced liver injury. Skin sensitivity is determined by the allergenic ability of a substance. The maximum recommended tolerated dose (MRTD) is an estimate of the highest concentration that can be given to animals (usually in preclinical studies) without causing substantial side effects. Therefore, an MRTD higher than 0.477 log (mg/kg/day) is thought to provide a good safety margin for drug candidates.

The oral rat acute (LD50) toxicity helps in determining the dosage of a substance estimated to be fatal when given to 50% of the test subjects. Likewise, in oral rat chronic (LOAEL) toxicity, the LOAEL determines the lowest dose at which observable adverse effects occur in the subjects. Hence, a lower LD50 value indicates a higher level of toxicity, whereas a higher LD50 value suggests lower acute toxicity. Here, adverse effects refer

to physiological changes, biochemical alterations, or any other signs of toxicity that may have a harmful effect on the health of the organism. Collectively, these assessments aid in identifying potential drug candidates

with optimal efficacy and safety profiles, guiding their progression through preclinical and clinical development stages.

**Table 3a: Selected ADME Properties of the Lead Compounds from the CID45242586 Library.**

Cmp ID	Absorption			Distribution		Metabolism		Excretion	
	Caco2	IA	SP (log Kp)	BBB (log BB)	CNS (log PS)	CYP1A2 inhibitor	CYP2C9 inhibitor	TCL (log ml/min/kg)	Renal OCT2 substrate
28230373	1.3	84.572	-2.735	0.499	-1.77	Yes	No	1.033	Yes
71797212	1.309	88.726	-2.735	0.515	-0.589	Yes	No	1.196	Yes
97104814	0.934	85.315	-2.375	0.216	-3.234	Yes	No	0.972	Yes
28360425	0.812	90.456	-2.735	-1.364	-3.762	No	No	0.812	No
31054613	1.41	94.406	-2.736	0.005	-2.392	Yes	Yes	0.997	Yes
76533214	1.103	89.07	-2.735	-1.03	-2.698	Yes	Yes	1.15	Yes
129067958	0.925	88.35	-2.735	0.012	-3.25	Yes	No	1.104	Yes
45179028	1.3	84.35	-2.735	0.499	-1.77	Yes	No	1.033	Yes
45185893	1.332	86.204	-2.735	0.509	-1.054	Yes	Yes	1.022	Yes
156276243	1.39	88.838	-2.735	0.462	-1.408	Yes	No	1.118	Yes

**Cmp ID** – compound ID; **Caco2** – permeability (log Papp in 10<sup>-6</sup> cm/s); **IA** – intestinal absorption (% absorbed); **SP** – skin permeability; **BBB** – blood–brain barrier permeability; **CNS** – central nervous system permeability; **TCL** – total clearance

Table 3a, together with Tables 3b, 4a, 4b, 5a, and 5b, present the ADME and toxicity studies of lead compounds from three libraries produced with the pkCSM online tool. These tables provide comprehensive insight into the pharmacokinetics and potential toxicity of the analyzed compounds. As shown in Table 3a, all the compounds in the CID45242586 library exhibited favorable permeability toward Caco2 cells as well as substantial intestinal absorption, suggesting that they can be readily absorbed through the gastrointestinal tract. Notably, all the compounds also demonstrated negligible skin penetration. The values of logBB for the BBB and

logPS for CNS permeability indicate that some compounds (e.g., 2, 8, 9, and 10) may have the ability to cross the BBB and permeate into the CNS. For the P450s, while the majority of them inhibit CYP1A2, except for a few, the remaining compounds have not shown any inhibitory effect on CYP2C9. In addition, while comparing the lead compounds, compound 2 can be considered to have a faster clearance, whereas compound 4 is found to exhibit a slower clearance. For the renal OCT2 substrate, except for compound 4, the other lead compounds acted as substrates.

**Table 3b: Toxicity Predictions for the Lead Compounds from the CID45242586 Library.**

Compound ID	AMES toxicity	Hepato-toxicity	Skin Sensitization	MRTD (mg/kg/day)	Oral Rat Acute Toxicity (LD50)	Oral Rat Chronic Toxicity (LOAEL)
28230373	Yes	No	No	0.054	2.711	1.303
71797212	Yes	Yes	No	0.478	2.357	1.583
97104814	Yes	Yes	No	-0.063	2.758	0.394
28360425	Yes	Yes	No	0.287	2.060	2.282
31054613	No	Yes	No	0.650	2.159	1.220
76533214	No	No	No	0.170	2.192	2.015
129067958	No	Yes	No	-0.075	2.205	0.501
45179028	Yes	No	No	0.054	2.711	1.303
45185893	No	Yes	No	0.026	2.151	1.449
156276243	Yes	Yes	No	-0.050	2.057	0.649

The toxicity predictions of the CID45242586 library are shown in Table 3b. With the exception of a few, the remaining compounds had a positive effect on both AMES and hepatotoxicity. However, none of these compounds are predicted to cause skin sensitization and thus do not pose any risk of allergic reactions upon skin exposure. Except for compounds 3, 7, and 10, the

remaining compounds are considered to exhibit moderate to high tolerance in terms of MRTD, suggesting that toxic effects can be observed only at comparatively higher doses. For acute and chronic toxicity, while all the compounds presented higher LD50 values, indicating lower acute toxicity, the LOAEL values showed that harmful effects can occur even at reasonably low doses.



**Table 4a: Selected ADME Properties of the Lead Compounds from the N(4)-OH-5-Fdcmp Library.**

Cmp ID	Absorption			Distribution		Metabolism		Excretion	
	Caco2	IA	SP (log Kp)	BBB (log BB)	CNS (log PS)	CYP1A2 inhibitor	CYP2C9 inhibitor	TCL (log ml/min/kg)	Renal OCT2 substrate
7058166	0.394	35.178	-2.735	-2.026	-3.755	No	No	-0.658	No
20056867	0.460	42.130	-2.736	-1.466	-3.606	No	No	-0.407	No
46936402	0.268	28.017	-2.735	-2.293	-4.485	No	No	0.246	No
46937009	0.455	16.509	-2.735	-1.814	-4.626	No	No	-0.077	No
25244665	0.344	34.099	-2.735	-2.07	-3.683	No	No	-0.589	No
447090	0.683	41.017	-2.745	-1.765	-3.892	No	No	-0.015	No
7058165	0.525	52.052	-2.735	-0.937	-3.456	No	No	-0.155	No
12358859	0.432	10.999	-2.735	-2.328	-4.741	No	No	-0.186	No
53840688	0.643	42.870	-2.735	-1.806	-3.815	No	No	0.031	No
25202302	0.319	43.854	-2.735	-2.231	-3.671	No	No	-0.629	No

**Cmp ID** – compound ID; **Caco2** – permeability (log Papp in 10–6 cm/s); **IA** – intestinal absorption (% absorbed); **SP** – skin permeability; **BBB** – blood–brain barrier permeability; **CNS** – central nervous system permeability; **TCL** – total clearance

The ADME properties of the lead compounds from the N(4)-OH-5-Fdcmp library are shown in Table 4a. The compounds in this library exhibited lower absorption than did the compounds from the CID45242586 library. All the compounds possessed only a lower Caco2 permeability, whereas excluding a few, the rest of the compounds showed promising absorption percentages (IA > 30%). Likewise, the values obtained for skin permeability suggest that these compounds cannot penetrate the skin. Most of these compounds have very little permeability toward the BBB or CNS, indicating

that all of these lead compounds can neither cross the BBB nor penetrate the CNS. In addition, these compounds had no inhibitory effect on CYP1A2 or CYP2C9. The TCL values ranging from -0.658 to 0.246 indicate efficient clearance of these compounds from the body. No compounds exhibit substrate properties for the renal OCT2. Overall, the ADME data suggest that compounds from this library exhibit more efficient pharmacokinetic profiles than compounds from the CID45242586 library.

**Table 4b: Toxicity Predictions for the Lead Compounds from the N(4)-OH-5-Fdcmp Library.**

Compound ID	AMES toxicity	Hepato-toxicity	Skin Sensitisation	MRTD (mg/kg/day)	Oral Rat Acute Toxicity (LD50)	Oral Rat Chronic Toxicity (LOAEL)
7058166	No	Yes	No	0.784	1.842	2.964
20056867	No	Yes	No	0.491	1.603	2.690
46936402	No	Yes	No	0.800	2.482	4.223
46937009	No	Yes	No	0.520	2.473	4.326
25244665	No	Yes	No	1.061	1.829	0.292
447090	No	Yes	No	0.584	2.296	2.526
7058165	No	Yes	No	0.264	1.503	2.431
12358859	No	No	No	0.486	2.476	5.030
53840688	No	Yes	No	0.457	2.389	2.340
25202302	No	Yes	No	0.819	1.859	0.293

In Table 4b, toxicity predictions for the compounds from the N(4)-OH-5-Fdcmp library are presented. Although most of the compounds were found to possess hepatotoxic effects, suggesting a potential risk to the liver, all the compounds had negative effects on AMES toxicity, confirming the absence of any mutagenic effects. As noted in the other two libraries, the lead compounds in this library also had negligible impacts on allergic reactions upon exposure to the skin. All the compounds are expected to have only moderate tolerance in the context of MRTD, suggesting that toxic effects will be observed even at relatively low doses. However, acute and chronic oral toxicity can occur at moderate to

low toxicity levels. Overall, while lead compounds exhibit some toxicity, further *in vitro* and *in vivo* studies are necessary to validate these predictions and ensure their safety for further development.

**Table 5a: Selected ADME Properties of the Lead Compounds from the Rheediaxanthone B Library.**

Cmp ID	Absorption			Distribution		Metabolism		Excretion	
	Caco2	IA	SP (log Kp)	BBB (log BB)	CNS (log PS)	CYP1A2 inhibitor	CYP2C9 inhibitor	TCL (log ml/min/kg)	Renal OCT2 substrate
73205	0.299	76.332	-2.735	-0.723	-2.821	No	No	0.075	No
10342859	0.178	100	-2.735	-0.987	-2.801	No	Yes	-0.777	No
52951054	0.611	84.85	-2.735	-1.225	-3.208	No	No	-0.065	No
195652	0.206	92.01	-2.736	-1.039	-2.054	No	Yes	0.112	No
11725803	0.299	76.332	-2.735	-0.723	-2.821	No	No	0.075	No
102060338	0.694	92.801	-2.827	-0.301	-1.718	Yes	Yes	0.005	No
10862711	1.258	94.153	-2.796	0.365	-1.899	Yes	Yes	-0.247	No
637252	0.064	70.624	-2.735	0.986	-2.875	No	No	0.215	No
10342859	0.178	100	-2.735	-0.429	-2.801	No	Yes	-0.777	No
15307925	0.697	93.865	-2.763	0.369	-1.69	Yes	Yes	-0.008	No

Cmp ID – compound ID; Caco2 – permeability (log Papp in 10<sup>-6</sup> cm/s); IA – intestinal absorption (% absorbed); SP – skin permeability; BBB – blood–brain barrier permeability; CNS – central nervous system permeability; TCL – total clearance

**Table 5b: Toxicity Predictions for the Lead Compounds from the Rheediaxanthone B library.**

Compound ID	AMES toxicity	Hepato-toxicity	Skin Sensitization	MRTD (mg/kg/day)	Oral Rat Acute Toxicity (LD50)	Oral Rat Chronic Toxicity (LOAEL)
73205	No	No	No	0.278	2.339	2.751
10342859	No	No	No	0.175	2.462	1.989
52951054	No	No	No	0.503	2.474	2.270
195652	No	Yes	No	0.267	2.499	1.891
11725803	No	No	No	0.278	2.339	2.751
102060338	No	Yes	No	-0.243	1.933	1.836
10862711	No	No	No	0.032	2.536	1.801
637252	No	No	No	0.405	2.316	2.948
10342859	No	No	No	0.175	2.462	1.989
15307925	No	No	No	-0.155	1.951	1.746

In Tables 5a and 5b, ADMET predictions and toxicity analysis results for the Rheediaxanthone B library are presented. These compounds have lower Caco2 permeability, as evidenced by their absorption values. In contrast, all the compounds exhibited substantial intestinal absorption with a negative impact on skin penetration. The BBB and CNS permeability values indicate that, except for compounds 7, 8, and 10 for the BBB and 6, 7, and 10 for the CNS, the other compounds have shown no propensity to cross the BBB or penetrate into the CNS. TCL values range from negative to positive, indicating that clearance rates differ among compounds. Although few compounds have demonstrated inhibitory potency against cytochrome P450 enzymes, none of the compounds showed substrate specificity for renal OCT2. According to the toxicity predictions (Table 5b), the compounds in this library exhibited little or no AMES toxicity, indicating the absence of any mutagenic potential. However, some compounds are predicted to be hepatotoxic, indicating possible liver damage upon exposure. Skin sensitization is not predicted among these compounds, suggesting that allergic reactions to skin contact are unlikely. As shown in the second library (Table 4b), the lead compounds in this library also exhibited moderate tolerance, suggesting that toxic effects can be observed at relatively low doses.

The acute and chronic oral toxicity tests showed moderate to low toxicity, confirming the expected safety standards.

## CONCLUSION

The present study successfully identified potential small molecule inhibitors of TS from specified compound libraries, including CID45242586, N(4)-OH-5-Fdcmp, and Rheediaxanthone B. The results of binding energy, physicochemical characteristic, ADME and toxicity prediction analyses of the three libraries provide valuable information needed for developing potential drug candidates against *T. spiralis*. The virtual screening docking results indicate promising binding energies for all leads, thus confirming the ability of these leads to inhibit *T. spiralis* TS and serve as effective drug candidates. Based on the analysis of their physicochemical properties, the majority of the lead compounds from all the libraries followed Lipinski's rule of five, indicating reliable drug likeness. Furthermore, these compounds have acceptable molecular weights, log Po/w values, topological polar surface areas, hydrogen bond acceptors, and donor counts, all of which suggest possible oral absorption and aqueous solubility. The evaluation of ADME characteristics provides information on the pharmacokinetic characteristics of the

lead compounds identified in each library. Different compounds have various characteristics related to absorption, distribution, metabolism, and excretion; however, certain compounds have certain features, including moderate to high absorption rates and restricted CNS penetration.

Toxicity predictions provide valuable information regarding the safety profiles of lead compounds. While most compounds demonstrate low mutagenic potential and minimal skin sensitization, certain compounds are predicted to have hepatotoxic effects. Acute and chronic oral toxicity values generally indicate moderate to low toxicity levels, with acceptable safety margins in the theoretical model. Hence, compounds exhibiting strong binding affinities and favorable pharmacokinetic profiles can be subjected to *in vitro* and *in vivo* validation studies to evaluate their efficacy, safety, and potency as therapeutic agents against *T. spiralis*. To summarize, the combination of virtual screening, physicochemical analysis, and ADMET prediction in the present study has facilitated the identification of small molecules that can inhibit *T. spiralis* TS. The promising leads presented here can be used for further R&D efforts in the search for an effective treatment for trichinellosis.

#### ACKNOWLEDGEMENT

The authors would like to acknowledge the support offered by Dr. Monika Chauhan, PhD, Program Director and Dr. Shashank Taxak, CEO, at Aitele Research LLP for providing essential resources and creating an environment conducive to research.

#### AUTHOR CONTRIBUTIONS

Conceptualization: LK; Software: UK; Investigation: UK; Methodology: UK; Formal Analysis: UK, LK; Writing - Original Draft Preparation: UK; Writing - Review & Editing: UK, LK; Supervision: LK.

#### CONFLICT OF INTEREST

The authors have no competing interests to declare.

#### FUNDING

No funding was received for this study.

#### DATA AVAILABILITY

The data supporting the findings of this study are available within the Results section of the manuscript.

#### ETHICS STATEMENT

Not applicable.

#### REFERENCES

- Adam Jarmuła, Piotr Wilk, Piotr Maj, Jan Ludwiczak, Anna Dowierciał, Katarzyna Banaszak, Wojciech Rypniewski, Joanna Cieśla, Magdalena Dąbrowska, Tomasz Frączyk, Agnieszka K. Bronowska, Jakub Jakowiecki, Sławomir Filipek, Wojciech Rode. Crystal structures of nematode (parasitic *T. spiralis* and free living *C. elegans*), compared to mammalian, thymidylate synthases (TS). Molecular docking and molecular dynamics simulations in search for nematode-specific inhibitors of TS. Journal of Molecular Graphics and Modelling, 2017; 77: 33–50.
- Kathryn J. Else, Jennifer Keiser, Celia V. Holland, Richard K. Grencis, David B. Sattelle, Ricardo T. Fujiwara, Lilian L. Bueno, Samuel O. Asaolu, Oluyomi A. Sowemimo, Philip J. Cooper. Whipworm and roundworm infections. Nature Reviews Disease Primers, 2020; 6(44).
- Thomson, P. D., & Smith Jr, D. J. What is infection? The American journal of surgery, 1994; 167(1): S7-S11.
- Antonovics Janis, Wilson Anthony J, Forbes Mark R, Haufler Heidi C, Kallio Eva R, Leggett Helen C, Longdon Ben, Okamura Beth, Sait Steven M, Webster Joanne P. The evolution of transmission mode. Phil. Trans. R. Soc. B, 2017; 372(1719).
- Dupouy-Camet J, Murrell KD. FAO/WHO/OIE guidelines for the surveillance, management, prevention, and control of trichinellosis. Parasite, 2007; 14(3): 196–203.
- K.D. Murrell, E. Pozio. Trichinellosis: the zoonosis that won't go quietly. International Journal for Parasitology, 2000; 30(12): 1339–1349.
- David B. Guiliano, Yelena Oksov, Sara Lustigman, Kleoniki Gounaris, Murray E. Selkirk. Characterisation of novel protein families secreted by muscle stage larvae of *Trichinella spiralis*. International Journal for Parasitology, 2009; 39(5): 515–524.
- Somnath W, Jaywant D, Shaha SY, Ramrao C. In Silico Homology Modeling of Thymidylate synthase from the nematode *Trichinella spiralis*. Drug Invention Today, 2011; 3(8).
- Garg D, Skouloubris S, Briffotiaux J, Myllykallio H, Wade RC. Conservation and Role of Electrostatics in Thymidylate Synthase. Sci Rep., 2015; 5(1): 17356.
- El Kouni MH. Pyrimidine metabolism in schistosomes: A comparison with other parasites and the search for potential chemotherapeutic targets. Comparative Biochemistry and Physiology Part B: Biochemistry and Molecular Biology, 2017; 213: 55–80.
- Rode W, Dąbrowska M, Zieliński Z. Gołos B, Wranicz M, Felczak K, Kulikowski T. *Trichinella spiralis* and *Trichinella pseudospiralis*: Developmental patterns of enzymes involved in thymidylate biosynthesis and pyrimidine salvage. Parasitology, 2000; 120: 593–600.
- M. Paola Costi, Donatella Tondi, Marcella Rinaldi, Daniela Barlocco, Piergiorgio Pecorari, Fabrizia Soragni, Alberto Venturelli, Robert M. Stroud. Structure-based studies on species-specific inhibition of thymidylate synthase. Biochimica et Biophysica Acta (BBA) - Molecular Basis of Disease, 2002; 1587(2): 206–214.

13. Rahman L, Voeller D, Rahman M, Lipkowitz S, Allegra C, Barrett JC, Kaye FJ, Zajac-Kaye M. Thymidylate synthase as an oncogene: a novel role for an essential DNA synthesis enzyme. *Cancer Cell*, 2004; 5: 341–351.
14. Kingsbury JM, Goldstein AL, McCusker JH. Role of nitrogen and carbon transport, regulation, and metabolism genes for *Saccharomyces cerevisiae* survival in vivo. *Eukaryot Cell*, 2006; 5: 816–824.
15. Kingsbury JM, McCusker JH. Homoserine toxicity in *Saccharomyces cerevisiae* and *Candida albicans* homoserine kinase (*thr1Δ*) mutants. *Eukaryot Cell*, 2010b; 9: 717–728.
16. Ramesh D, Joji A, Vijayakumar BG, Sethumadhavan A, Mani M, Kannan T. Indole chalcones: Design, synthesis, in vitro and in silico evaluation against *Mycobacterium tuberculosis*. *European Journal of Medicinal Chemistry*, 2020; 198: 112358.
17. Maj P, Mori M, Sobich J, Markowicz J, Uram Ł, Zieliński Z, Quaglio D, Calcaterra A, Cau Y, Botta B, Rode W. Alvaxanthone, a Thymidylate Synthase Inhibitor with Nematocidal and Tumoricidal Activities. *Molecules*, 2020; 25(12): 2894.
18. Rode W, Zieliński Z, Dzik JM, Kulikowski T, Bretner M, Kierdaszuk B, Cieśla J, Shugar D. Mechanism of inhibition of mammalian tumor and other thymidylate synthases by N4-hydroxy-dCMP, N4-hydroxy-5-fluoro-dCMP, and related analogues. *Biochemistry*, 1990; 29(48): 10835–10842.
19. Dallakyan S, Olson AJ. Small-molecule library screening by docking with PyRx. *Methods Mol. Biol.*, 2015; 1263: 243–250.
20. Goddard TD, Huang CC, Meng EC, Pettersen EF, Couch GS, Morris JH, Ferrin TE. UCSF ChimeraX: Meeting modern challenges in visualization and analysis. *Protein Sci.*, 2018; 27(1): 14–25.
21. Dassault Systèmes BIOVIA, Discovery Studio Visualizer, v20.1.0.19295, San Diego: Dassault Systèmes 2020.
22. Daina A, Michielin O, Zoete V. SwissADME: a free web tool to evaluate pharmacokinetics, drug-likeness and medicinal chemistry friendliness of small molecules. *Scientific Reports*, 2017; 7(1): 42717.
23. Pires DE, Blundell, TL. Ascher DB. pkCSM: predicting small-molecule pharmacokinetic and toxicity properties using graph-based signatures. *Journal of Medicinal Chemistry*, 2015; 58(9): 4066–4072.
24. Alex M Clark, Krishna Dole, Anna Coulon-Spektor, Andrew McNutt, George Grass, Joel S. Freundlich, Robert C. Reynolds, Sean Ekins. Open Source Bayesian Models. 1. Application to ADME/Tox and Drug Discovery Datasets. *J. Chem. Inf. Model*, 2015; 55(6): 1231–1245.